FREQUENCY DOMAIN MEASUREMENTS OF THE FLUORESCENCE LIFETIME OF RIBONUCLEASE T_1

MAURICE R. EFTINK AND CAMILLO A. GHIRON
Department of Chemistry, The University of Mississippi, University, Mississippi 38677; and
Department of Biochemistry, The University of Missouri, Columbia, Missouri 65201

ABSTRACT Using multifrequency phase/modulation fluorometry, we have studied the fluorescence decay of the single tryptophan residue of ribonuclease T_1 (RNase T_1). At neutral pH (7.4) we find that the decay is a double exponential ($\tau_1 = 3.74$ ns, $\tau_2 = 1.06$ ns, $f_1 = 0.945$), in agreement with results from pulsed fluorometry. At pH 5.5 the decay is well described by a single decay time ($\tau = 3.8$ ns). Alternatively, we have fitted the frequency domain data by a distribution of lifetimes. Temperature dependence studies were performed. If analyzed via a double exponential model, the activation energy for the inverse of the short lifetime component (at pH 7.4) is found to be 3.6 kcal/mol, as compared with a value of 1.0 kcal/mol for the activation energy of the inverse of the long lifetime component. If analyzed via the distribution model, the width of the distribution is found to increase at higher temperature. We have also repeated, using lifetime measurements, the temperature dependence of the acrylamide quenching of the fluorescence of RNase T_1 at pH 5.5. We find an activation energy of 8 kcal/mol for acrylamide quenching, in agreement with our earlier report.

There have been several important studies dealing with the fluorescence of the single tryptophanyl residue of ribonuclease T_1 (RNase T_1) from *Aspergillus oryzae*. Longworth (1) observed that the tryptophanyl fluorescence of this protein occurs at a lower maximum wavelength ($\lambda_{max} \sim 325$ nm) than most tryptophanyl residues in proteins. Also he found that the emission of RNase T_1 shows a noticeable degree of vibrational fine structure, which is unusual for proteins. These findings suggested that Trp-59 of RNase T_1 is buried in a nonpolar region in this small, globular protein. Eftink and Ghiron (2) then found that the fluorescence of RNase T_1 can be quenched by acrylamide, but with a quenching rate constant that is small compared with other tryptophanyl residues in proteins. Furthermore, the temperature and viscosity dependencies of the acrylamide quenching of RNase T_1 were found to be quite different than that for the acrylamide quenching of indole or surface tryptophanyl residues (2–4). These temperature and viscosity dependencies have been interpreted as indicating that fluctuations in the structure of the protein are required for acrylamide to strike the buried Trp-59. Other quenching studies have shown that Trp-59 of RNase T_1 is almost completely shielded from the charged quencher, iodide, and that it can be quenched with a moderate rate constant by the small, nonpolar quencher, oxygen (5, 6).

Anisotropy decay studies and lifetime resolved anisotropy studies show that Trp-59 is relatively immobilized within the globular protein (5–8).

The crystal structure of an RNase T_1-2′-GMP complex provides a reasonable rationalization of these fluorescence findings (9). Trp-59 is located beneath the surface of the protein and is flanked by nonpolar residues of proline, tyrosine, and phenylalanine (8, 9).

The fluorescence of RNase T_1 continues to be an important topic. Recent single photon-counting measurements by Chen et al. (8) indicate that the fluorescence decay of Trp-59 is not a single exponential at neutral pH.

In this manuscript we report multifrequency phase/modulation measurements of the fluorescence of RNase T_1. Our data generally support the pulse-decay measurements of Chen et al. (8), yet we also find that the lifetime distribution model of Gratton et al. (10) provides a fit to the data that is difficult to distinguish from a double exponential fit. Also we report temperature and viscosity dependence studies, using fluorescence lifetime measurements, of the acrylamide quenching of RNase T_1.

MATERIALS AND METHODS

Ribonuclease T_1 was obtained from Dr. F. Walz, Jr., Kent State University, as a lyophilized sample. Acrylamide was recrystallized from ethyl acetate. Spectral grade glycerol was obtained from Aldrich Chemical Co., Milwaukee, WI. Sodium acetate and sodium phosphates, used for buffers, were reagent grade. Distilled, deionized water was used.

Phase/modulation fluorescence lifetimes were obtained with a SLM-4800 C fluorometer (SLM-Aminco Inc., Urbana, IL), equipped with a multifrequency light modulator from ISS Inc., Champaign, IL. This instrument uses a xenon arc lamp and a pockels cell light modulator (driven at frequencies ranging from 10 to 200 MHz). A 10-nm-wide interference filter (Melles Griot, Irvine, CA), centered at 290 nm, was used to select the excitation wavelength. Emission was observed through a 7–60 filter (Corning Glassworks, Corning, NY). The photomultiplier tubes (Hamamatsu Corp., Middlesex, NJ) were also modulated in the megahertz range and with a cross-correlation frequency of 25 Hz. The photomultiplier amplifiers are interfaced with a 158 computer (Zenith Controls, Inc., Chicago, IL) and software, obtained from ISS Inc., was used to acquire and perform least squares analyses of the data. This software fits one or two component decay kinetics to the multifrequency phase and modulation data (11). In addition to fitting discrete lifetime

(i.e., one or two components) models to the data, a lifetime distribution (Lorentzian) analysis was also performed.

Apparent phase-($\tau_{p,\omega}$) and modulation-lifetimes ($\tau_{m,\omega}$), and the raw-phase angle, Φ_ω, and relative modulation, M_ω, were obtained by making ~ 20 2.5-s measurements at each frequency, ω. Typical standard deviations were 0.5% and 0.2% for $\tau_{p,\omega}$ and $\tau_{m,\omega}$. *p*-Terphenyl in ethanol was used to provide a reference lifetime (12). The protein sample generally had an absorbance of <0.10 at 290 nm. Temperature was maintained with a water bath, which circulated water through the cell holder.

Phase resolved spectra were obtained with a modified arrangement of the above equipment. A 450-W Xenon arc served as the light source and a Debye-Sears modulator tank was used to modulate the light at 30 MHz. Again a 290-nm interference filter was used on the excitation side, but a monochromater was placed on the emission side. An EMI photomultiplier (also modulated at 30 MHz) was used. After measuring phase angle and relative modulation values across the emission band, the fluorescence lifetimes for the two component fit were used to calculate the spectra of each component (13).

RESULTS

In Fig. 1 *A* is shown a multifrequency measurement of the phase angle and relative modulation of the fluorescence of RNase T_1 at 15°C and pH 7.4 (Tris buffer). Shown are a one-component and a two-component fit to the data. Clearly the two-component fit is superior (lower reduced chi squared, χ^2). The best fit is $\tau_1 = 3.74$ ns, $\tau_2 = 1.06$ ns, $f_1 = 0.945$, and $f_2 = 0.055$. These values are in excellent agreement with values recently reported by Chen et al. (8), who used a pulsed single-photon counting method.

Similar measurements were made at pH 5.5, as shown in Fig. 2. At this pH the χ^2 for a one-component fit ($\tau = 3.80$ ns) is somewhat (about threefold) larger than that for a two-component fit, but the former fit is judged to be adequate. On comparing the fits at pH 7.4 and 5.5, it is clear that the fluorescence decay at pH 5.5 is more nearly characterized as being a single exponential. In Tables I and II are shown the best fits to frequency domain data at pH

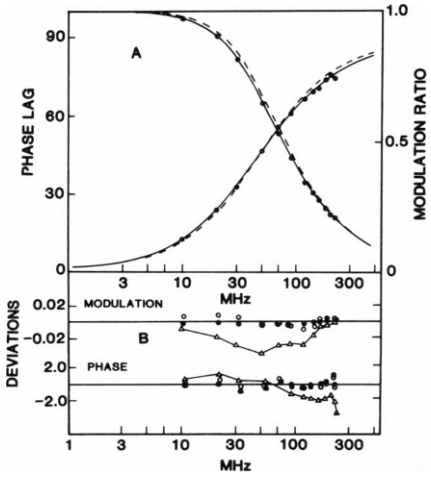

FIGURE 1 (*A*) Multifrequency phase/modulation data for RNase T_1 at pH 7.4, 15°C. The solid line is a double exponential fit with $\tau_1 = 3.74$ ns, $f_1 = 0.945$, and $\tau_2 = 1.06$ ns. The dashed line shows the best single-component fit ($\tau = 3.35$ ns). (*B*) Deviation pattern for the single component (△), double component (●), and distribution (○) fits.

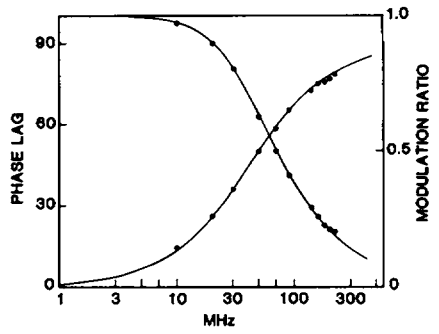

FIGURE 2 Multifrequency phase-modulation data for RNase T_1 at pH 5.5, 15°C. The solid line is the best single-component fit with $\tau = 3.80$ ns.

7.4 and 5.5, respectively, for RNase T_1 at various temperatures.[1] For the pH 5.5 data there is, on average, about a fourfold reduction in χ^2 on going from a one-component to a two-component fit. This relative drop in χ^2 is consistently smaller than the ninefold drop (average) observed at pH 7.4.

These data were also analyzed via a continuous distribution model (10). As shown in Fig. 3, a good fit is obtained with a Lorentzian distribution centered aroung 3.5 ns (at pH 7.4) or 3.9 ns (at pH 5.5) for the data at 15°C. For the data at pH 7.4 the halfwidth of the distribution is 0.63 ns. This is significantly greater than the halfwidth of 0.27 ns at pH 5.5. For comparison, data for indole in water, which presumably decays as a single exponential, shows a halfwidth of ~ 0.1 ns upon analysis in this manner.

We also performed a few studies in a 0.03-M sodium phosphate buffer at pH 7.2. With this buffer the decay appears to be described reasonably well as a single exponential (i.e., at 10°C, we obtain a single component fit of $\tau_1 = 2.98$ ns, $\chi^2 = 25.7$ and a two-component fit of $\tau_1 = 3.20$, $\tau_2 = 0.91$, $f_1 = 0.96$, $\chi^2 = 5.8$). The difference between phosphate and Tris buffer is probably due to the fact that phosphate binds at the enzyme's active site.

In an attempt to obtain further evidence for or against the discrete lifetimes interpretation, we have studied the temperature dependence of the τ_i for RNase T_1 at pH 7.4. Shown in Fig. 4 is an Arrhenius plot of $1/\tau_1$ and $1/\tau_2$ values obtained between 1 and 50°C. There is a much greater variability in the short lifetime data, but it is quite clear that the activation energy, E_a, for the fluorescence lifetime of each putative component is quite different. We

[1]We note that the χ^2 values may seem unusually large. This is because we have used standard deviations of 0.20 and 0.004 for the phase angle and relative modulation measurements, respectively. Actually the standard deviations for our phase angle and modulation measurements were ~ 0.50 and 0.005, respectively. With these values, χ^2 are calculated to be in the range of 1–3, a range which is expected for a proper fit. Nevertheless, the χ^2 values that we list in Tables I and II are good for comparative purposes. The ISS Inc. software employed for the distribution analysis uses default standard deviations of 0.20 and 0.004 for the phase and modulation. Thus all the χ^2 in Tables I and II are relative to one another.

TABLE I
LIFETIME ANALYSES FOR RNase T_1 AT pH 7.4

Temperature	Single-component fit		Two-component fit				Lorentzian distribution fit		
	τ_1	χ^2	τ_1	τ_2	f_1	χ^2	Center	Width	χ^2
°C	*ns*		*ns*				*ns*		
1.1	3.76	30.6	4.24	1.70	0.903	4.4	3.90	0.55	3.4
4.6	3.55	49.5	3.98	1.17	0.938	4.6	3.74	0.68	5.9
10.3	3.42	52.2	3.99	1.53	0.887	11.2	3.61	0.65	9.3
14.9	3.35	48.1	3.74	1.06	0.945	7.4	3.53	0.63	7.1
20.0	3.38	58.6	3.68	0.73	0.963	13.1	3.54	0.70	11.5
25.0	3.18	64.7	3.62	1.01	0.936	7.8	3.38	0.70	8.7
29.7	3.01	104.8	3.57	0.98	0.911	12.3	3.24	0.92	14.8
34.5	2.92	107.2	3.43	0.85	0.925	4.6	3.15	0.92	7.9
39.3	2.80	150.1	3.23	0.44	0.948	6.8	3.03	1.08	17.6
44.2	2.82	63.6	3.17	0.71	0.898	10.3	2.95	1.11	9.0
50.5	2.72	132.6	3.11	0.60	0.932	28.0	2.84	0.92	26.2

TABLE II
LIFETIME ANALYSES FOR RNase T_1 AT pH 5.5

Temperature	Single-component fit		Two-component fit				Lorentzian distribution fit		
	τ_1	χ^2	τ_1	τ_2	f_1	χ^2	Center	Width	χ^2
°C	*ns*		*ns*				*ns*		
1.1	3.93	18.5	4.77	2.70	0.709	3.8	4.04	0.45	3.3
6	4.07	13.1	4.29	2.67	0.886	12.6	4.09	0.28	15.6
10	3.90	20.3	4.12	0.97	0.974	3.7	4.01	0.44	3.3
15	3.80	10.6	3.97	1.31	0.971	3.2	3.87	0.27	3.1
20	3.65	24.1	4.07	1.78	0.901	7.4	3.76	0.42	7.2
25	3.53	20.1	4.00	1.43	0.912	5.7	3.64	0.43	6.0
34	3.26	28.6	3.62	1.31	0.926	4.2	3.39	0.47	3.9
44	2.98	25.8	4.64	2.47	0.363	6.4	3.07	0.32	11.0
50.5	2.81	61.8	3.63	1.69	0.722	10.9	2.94	0.65	11.2

obtain $E_{a,1} = 1.03 \pm 0.05$ kcal/mol and $E_{a,2} = 3.6 \pm 0.8$ kcal/mol. We note that f_1 remained nearly constant throughout the temperature range.

Alternately, the temperature dependence of the frequency domain data can be interpreted by analysis of the data via the Lorentzian distribution model (see Fig. 5). At pH 7.4 the halfwidth of the distribution is observed to increase from 0.55 ns at 1.1°C to ~ 1 ns at 40°–50°C. At pH 5.5, the halfwidth of the distribution is smaller at all temperatures, and shows no significant change with temperature from 0° to 50°C.

We have repeated our temperature dependence study of the acrylamide quenching of RNase T_1 (2). In our earlier work, steady-state measurements were made. Since it is possible that static quenching can interfere with such measurements, we hoped to eliminate this concern by making lifetime measurements. We also selected pH 5.5 for our study, since the fluorescence appears to be more nearly a single exponential at this pH. Shown in Fig. 6 is an Arrhenius plot of the rate constant for acrylamide quenching over the temperature range of 1°–45°C. The activation energy that we find is 8.0 ± 1.0 kcal/mol, which is in excellent agreement with our previously determined value.

The acrylamide quenching rate constant has also been determined in a 50% (wt/wt) glycerol solution (pH 5.5 acetate buffer) at 6°C. From lifetime measurements, the acrylamide quenching-rate constant for the tryptophan in RNase T_1 is $5.7 \times 10^7\ M^{-1}\ s^{-1}$. Single component fits were

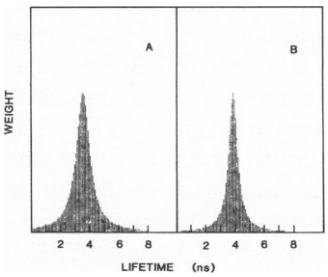

FIGURE 3 Lorentzian distribution fits to the data in Figs. 1 and 2. (*A*) Data at pH 7.4; (*B*) data at pH 5.5. Tables I and II give the fitting parameters.

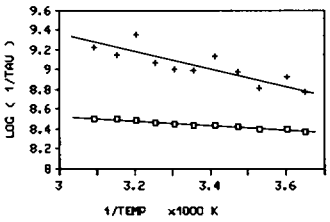

FIGURE 4 Arrhenius plot of the τ_1 (□) and τ_2 (+) for RNase T_1 at pH 7.4.

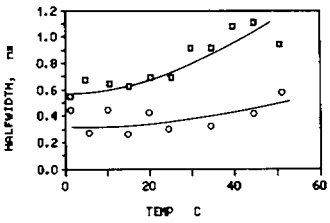

FIGURE 5 Temperature dependence of the width of the distribution fit for RNase T_1 at pH 7.4 (□) and pH 5.5 (○). The lines have no theoretical significance.

found to be adequate for samples containing 0, 1, and 2 M acrylamide.

DISCUSSION

Fluorescence Lifetime Studies

The fluorescence decay of the single tryptophanyl residue in RNase T_1 is slightly nonexponential at neutral pH. This fact had been previously noted by Grinvald and Steinberg (14) and more recently by Chen et al. (8). The latter group used a pulsed fluorometer and fitted the decay to a double exponential at pH 7.4, a major component ($f_1 = 0.908$) with $\tau_1 = 3.95$ ns and a minor component ($f_2 = 0.092$) with $\tau_2 = 1.6$ ns. Using multifrequency phase-modulation fluorometry we here obtain nearly the same analysis of the fluorescence of RNase T_1. Only in recent years has it become possible to obtain multifrequency phase-modulation lifetimes and to thus analyze nonexponential decays (10, 11, 15, 16). The close agreement between time domain and frequency domain measurements, on a protein sample from the same source, demonstrates that the latter method is capable of equaling the former method in its resolving power.

A point has recently been raised, by the laboratories of Ware (17), Albery (18), and Gratton (10), that the fluorescence decay of fluorophores in structured systems (i.e., proteins) may be better described by some type of distribution of decay times. An indole ring in a protein may experience a set of different microenvironments, due, for example, to the existence of various rotational (i.e., of the tryptophan side chain and neighboring amino-acid side chains) conformers or various structures having a different distance between the indole ring and a quenching side chain (i.e., the side chains of His, Lys, Met, and Cys). If the indole ring were to rapidly sample all possible microenvironments, the decay would be exponential. If, however, the conformational fluctuations (i.e., side chain rotations and intramolecular motions) are slower than, or on the same time scale as, the average decay time, then a multiexponential decay may result and some type of continuous distribution of fluorescence lifetimes may be a reasonable description of the kinetic pattern.

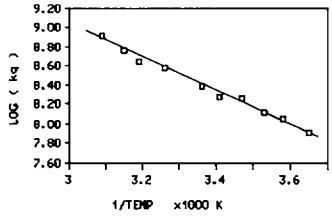

FIGURE 6 Arrhenius plot for the acrylamide quenching rate constant, k_q, for RNase T_1 at pH 5.5. k_q values obtained from fluorescence lifetime measurements made at 30 MHz, in the absence and presence of 0.5 and 1.0 M acrylamide.

The suggestion that the fluorescence of single tryptophan residues in proteins be described as a continuous distribution has sparked much interest and debate. We show that for RNase T_1 at pH 7.4 one can fit frequency domain data with either a Lorentzian distribution or with two discrete decay times. Obviously the question of which type of fit is most realistic is a very important one to answer for RNase T_1 and proteins in general. Also, other distribution shapes may be more appropriate, as has been discussed by Alcala et al. (19, 20). We have, for example, fitted the RNase T_1 data to a Gaussian distribution; the fits are qualitatively similar to the Lorentzian fits presented here. The important question at this time is whether a distribution model or discrete lifetime model provides the most realistic fit for the fluorescence decay of proteins.

Chen et al. (8) have argued that there is good reason to favor the two discrete lifetime fit for RNase T_1. They showed that the nonexponentiality appears only above pH 6.5–7; at pH 5.5–6 they found that a single component fit is adequate. Our frequency domain results are in general support of their finding. These results suggest that the deprotonation of some group on the enzyme is responsible for the change in the decay pattern, and Chen et al. proposed that two different conformational states (different conformations with respect to the microenvironment of Trp-59, i.e., in the minor state the trp must undergo additional dynamic quenching) exist above pH 7. Support for this proposal comes from acrylamide quenching results, which show that the short and long lifetimes have different quenching rate constants. The rate constant for acrylamide quenching of the short lifetime component is about six times larger than that for the major, long lifetime component.

Our finding of different activation energies for the thermal quenching of the two discrete components can be taken as support for the double exponential fit. The E_a for the long component is low, 1.03 kcal/mol. This value is similar to that found for other buried tryptophanyl residues in proteins (21, 22) and presumably reflects the nonpolar and/or relatively rigid microenvironment around the tryptophanyl residue. The E_a value at pH 5.5 for the single component fit is similar to the value for the long component at pH 7.4. The E_a for the short lifetime component (at pH 7.4), however, is significantly larger, 3.6 kcal/mol. The larger E_a suggests that this tryptophan "state" experiences thermally activated quenching processes. These may involve collisions with nearby peptide bonds or quenching side chains. Such collisions would lead to both the higher E_a and lower lifetime. The larger acrylamide quenching rate constant for this component is again consistent with the enhanced mobility of this "state" and with the possible location of the indole side chain closer to the surface of the protein. The fractional contribution of this minor component does not change significantly from 1° to 50°C. This

can be explained by the fact that, at a pH of 7.4, the ionizing group is nearly fully unprotonated at all temperatures and the proposal that the equilibrium between the two states (i.e., the long lifetime state and the short lifetime state) is temperature independent.

However it is not clear that the two discrete lifetime fit is superior to the distribution analysis. Fig. 1 *B* shows that the error profile is similar for the best fits with each model. Instead of discussing two activation energies for the two putative components, one could explain the temperature dependence in terms of an increase in the halfwidth of the distribution as temperature increases. In the latter case the increase in distribution width at a higher temperature may indicate that a wider distribution of microstates (i.e., slightly different conformations) is populated at higher temperature. Gratton et al. (10) have recently reported the opposite temperature dependence of the distribution width of RNase T_1 under somewhat different conditions. We cannot explain the difference in our observations, but Gratton et al. focused primarily on temperatures below 0°C, whereas we have studied only temperatures above 0°C.

To judge whether our least squares analyses can distinguish between a Lorentzian distribution and two discrete lifetimes, we performed a simulation in which we started with pseudo-Lorentzian synthetic data and fitted the two models. The synthetic data consisted of a distribution of seven lifetimes, centered at 3 ns, with pre-exponential weights corresponding to a Lorentzian shape of full-width-half-max equal to 1.0 ns (see Fig. 7 *A*). We calculated the theoretical phase angles and modulation ratios for this distribution. After introducing a 1% random error in these synthetic phase and modulation data, we performed least squares analyses of the data via the double exponential and Lorentzian distribution models. Fig. 7, *B* and *C* shows the resulting fits and the error patterns. Interestingly, the two discrete lifetime fit shows a major component that is larger than the true average lifetime, and a 30% minor component at a lower lifetime. This simulation calls into question the above two discrete lifetime fit for RNase T_1. The two component analyses for RNase T_1 show a 5–10% short lifetime component. Our simulation demonstrates that such a minor, short lifetime component would result if a double exponential fit were applied to data that should actually be a Lorentzian distribution.

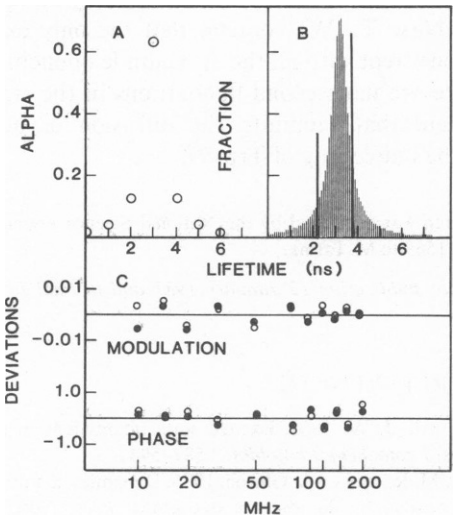

FIGURE 7 (*A*) Set of lifetimes used to simulate a pseudo-Lorentzian distribution. (*B*) Fit of synthetic data to a Lorentzian distribution (*shaded area*) and a double exponential decay (*solid lines*). (*C*) Comparison of the error (experimental minus calculated value) patterns for distribution (○) and double exponential (●) fits.

We have also performed this simulation for the situation in which a dynamic quencher (i.e., acrylamide) is added. In this simulation we allowed the lifetime and fractional contribution (but the pre-exponential, α, value remained constant) for each of the seven components in Fig. 7 *A* to change in response to the addition of quencher (we assumed the same quenching rate constant for each component). The synthetic data were then analyzed as above. The distribution analysis showed the expected decrease in both the center and width of the distribution. The two-component fit was again reasonable and showed both lifetimes to decrease, yet the proportion of the shorter lifetime was found to increase (compared with its α_i or f_i in the absence of quencher). Reflecting back to the acrylamide quenching study of Chen et al. (8), they reported that the lifetime of the putative minor component of RNase T_1 is decreased, proportionally, more by the addition of acrylamide than is the lifetime of the long lifetime component. This observation is the only one that cannot be easily explained in terms of a distribution model, for it would actually correspond to a broadening of the distribution upon the addition of quencher. In other words, the preferential quenching of the short lifetime component is, in our opinion, the strongest argument to support their two discrete lifetime analysis. We must point out, however, that we have considered only a Lorentzian distribution; other distribution shapes may allow the explanation of the data for the acrylamide quenching of RNase T_1.

In summary, both the two-component and distribution analysis can provide good fits to the lifetime data for RNase T_1. It will be difficult to distinguish such fits on statistical grounds.

We attempted to resolve the emission spectra of the putative two components using the phase resolved method of Jameson and Gratton (13). However, the contribution of the minor component is so small that we could not manage a separation of the components. Chen et al. also noted that they were unable to obtain a resolution of the two components by monitoring the emission decay at various wavelengths.

Acrylamide Quenching Studies

Since the fluorescence decay is now known to be nonexponential at neutral pH, we have repeated at pH 5.5 some of

our studies of the temperature and viscosity dependence of acrylamide quenching of the buried Trp-59. This was done to minimize any complications due to the complex decay at neutral pH, where our previous studies were performed. The activation energy for acrylamide quenching is again found to be 8 ± 1 kcal/mol. As we argued before (2, 3), this E_a is significantly larger than the E_a expected for the diffusion of acrylamide through water. This indicates that conformational fluctuations in the protein must occur (characterized by an E_a of 8 kcal/mol) in order to facilitate the quenching process. Also the Arrhenius plot is found to be linear over a very broad temperature range. This indicates that an unfolding mechanism, or a competing quenching mechanism with a different temperature dependence, is not kinetically important.

Also the relative insensitivity of the acrylamide quenching process to bulk viscosity is again demonstrated. At 6°C and 50% glycerol, the ratio of T/η (where η is the bulk viscosity) is 12.5-fold lower than the T/η value for water at 25°C. According to the Stokes-Einstein relationship, one would then expect a 12.5-fold lower k_q in the low temperature–50% glycerol solution. However, only a 3.8-fold reduction in k_q is observed, compared with the 25°C–water value. Thus the acrylamide quenching process must not be limited by the diffusion of acrylamide through the bulk medium. The quenching process must also be limited by fluctuations in the conformation of the protein which are required to facilitate the quenching process and which are relatively insensitive to the bulk viscosity (3, 4, 23).

Several years ago we suggested that the quenching by acrylamide of internal tryptophanyl residues in proteins can involve the penetration of the quencher into the globular structure, this penetration being facilitated by fluctuations, on the nanosecond time scale, in the structure of the protein. A similar process had been proposed to explain oxygen quenching of proteins (24). However, some researchers have offered other explanations for the acrylamide quenching data, probably because acrylamide is larger than oxygen and there is some reluctance to accept the explanation that "holes" the size of acrylamide move about in proteins. A protein unfolding model has been promoted by Englander, Vanderkooi, and co-workers (25). Recently Chen et al. (8) have suggested that acrylamide may quench by an electron transfer process over a distance (i.e., no contact with the indole ring required). There has been much interest in electron transfer processes in proteins (26), and the implications of an electron tunnelling mechanism of solute quenching must be considered. Also the possibility of Forster energy transfer quenching has been raised (25). We recognize that these alternate mechanisms have been proposed, but it is our opinion that the mechanism that is most consistent with the entire body of data, for the acrylamide quenching of buried tryptophans such as that in RNase T_1 and cod parvalbumin, is the penetration model. The unfolding, electron transfer over a distance, and energy transfer mechanisms each fail to account for the relative viscosity independence of acrylamide quenching. For each of these models, something approaching Stokes-Einstein behavior would be expected. Only the penetration model accounts for the relative independence of the acrylamide k_q on bulk viscosity for internal tryptophanyl residues (4). Likewise the relatively large E_a for acrylamide quenching is readily interpreted with the penetration model, which is not the case for the other models (i.e., the unfolding model would predict a very large E_a, and the energy transfer model would predict an E_a value corresponding to diffusion through water). Also, studies with the inefficient quencher succinimide (27), and a comparison of the quenching of internal tryptophanyl residues by various different efficient quenchers (i.e., O_2 quenches RNase T_1 better than acrylamide; iodide quenches much worse [5, 6]) clearly are inconsistent with the unfolding model. Finally, studies of the acrylamide quenching of indole and *N*-acetyl-L-tryptophanamide show that the effective encounter distance for quenching is approximately equal to the van der Waals contact distance for the reactants (28, 29). The mechanism of acrylamide quenching of indole fluorescence is most likely an electron transfer process (29), but the model systems studies show that quenching apparently requires physical contact between the quencher and the excited state, and that reaction beyond the immediate solvation layer is not kinetically important.

Our frequency domain data with RNase T_1 support the results of Chen et al. at pH 5.5 and 7.4. We have found the activation energies for the thermal quenching of the two decay times at pH 7.4 to be different. However we find that a Lorentzian distribution model also provides a reasonable fit to the frequency domain data for RNase T_1 at various temperatures. We have repeated important viscosity and temperature dependence studies of the acrylamide quenching of RNase T_1. We contend that the only explanation that is consistent with all the acrylamide quenching data is that there are nanosecond fluctuations in the structure of the protein that facilitate the diffusion of acrylamide toward the indole ring of Trp-59.

This research was supported by the National Science Foundation grant DMB 85-11569 to M. Eftink.

Received for publication 12 January 1987 and in final form 19 May 1987.

REFERENCES

1. Longworth, J. W. 1968. Excited state interactions in macromolecules. *Photochem. Photobiol.* 7:587–594.
2. Eftink, M. R., and C. A. Ghiron. 1975. Dynamics of a protein matrix as revealed by fluorescence quenching. *Proc. Natl. Acad. Sci. USA.* 72:3290–3294.
3. Eftink, M. R., and C. A. Ghiron. 1977. Exposure of tryptophanyl residues and protein dynamics. *Biochemistry.* 16:5546–5551.
4. Eftink, M. R., and K. A. Hagaman. 1986. The viscosity dependence of the acrylamide quenching of the buried tryptophan residue in parvalbumin and ribonuclease T_1. *Biophys. Chem.* 25:277–282.

5. Lakowicz, J. R., B. P. Maliwal, H. Cherek, and A. Balter. 1983. Rotational freedom of tryptophan residues in proteins and peptides. *Biochemistry*. 22:1741–1752.
6. James, D. R., D. R. Demmer, R. P. Steer, and R. E. Verrall. 1985. Fluorescence lifetime quenching and anisotropy studies in ribonuclease T_1. *Biochemistry*. 24:5517–5526.
7. Eftink, M. R. 1983. Quenching resolved fluorescence anisotropy studies with single and multi-tryptophan containing proteins. *Biophys. J.* 43:323–334.
8. Chen, L. S., J. W. Longworth, and G. R. Fleming. 1987. Picosecond time resolved fluorescence of ribonuclease T_1: a pH and substrate-analog binding study. *Biophys. J.* 51:865–873.
9. Heinemann, U., and W. Saenger. 1982. Specific protein-nucleic acid recognition in ribonuclease T_1-2'-guanylic acid complex: an x-ray study. *Nature (Lond.)*. 299:27–31.
10. Gratton, E. 1987. Fluorescence lifetime distributions in proteins. Proceeding of the International Symposium. Fluorescent Biomolecules: Methodologies and Applications. In press.
11. Gratton, E., M. Limkeman, J. R. Lakowicz, B. P. Maliwal, H. Cherek, and G. Laczko. 1984. Resolution of mixtures of fluorophores using variable-frequency phase and modulation data. *Biophys. J.* 46:479–486.
12. Lakowicz, J. R., H. Cherek, and A. Balter. 1981. Correction of timing errors in photomultiplier tubes used in phase and modulation fluorometry. *J. Biochem. Biophys. Methods*. 5:131–146.
13. Gratton, E., and D. M. Jameson. 1985. New approach to phase and modulation resolved spectra. *Anal. Chem.* 57:1694–1697.
14. Grinvald, A., and I. Z. Steinberg. 1976. The fluorescence decay of tryptophan residues in native and denatured proteins. *Biochim. Biophys. Acta*. 427:663–678.
15. Gratton, E., and M. Limkeman. 1983. A continuously variable frequency cross-correlation phase fluorometer with picosecond resolution. *Biophys. J.* 44:315–324.
16. Lakowicz, J. R., and B. P. Maliwal. 1985. Construction and performance of a variable-frequency phase-modulation fluorometer. *Biophys. Chem.* 21:61–78.
17. James, D. R., and W. R. Ware. 1985. A fallacy in the interpretation of fluorescence decay parameters. *Chem. Phys. Lett.* 120:455–462.
18. Albery, W. J., P. N. Bartlett, C. P. Wilde, and J. R. Darwent. 1985. A general model for dispersed kinetics in heterogeneous systems. *J. Am. Chem. Soc.* 107:1854–1858.
19. Alacala, J. R., E. Gratton, and F. G. Prendergast. 1987. Resolvability of fluorescence lifetime distributions using phase fluorometry. *Biophys. J.* 51:587–596
20. Alcala, J. R., E. Gratton, and F. G. Prendergast. 1987. Fluoresence lifetime distributions in proteins. *Biophys. J.* 51:597–604.
21. Szabo, A. G., T. M. Stepanik, D. M. Wagner, and N. M. Young. 1983. Conformational heterogeneity of the copper binding site in azurin. *Biophys. J.* 41:233–244.
22. Eftink, M. R., and K. A. Hagaman. 1985. Fluorescence quenching of the buried tryptophan residue in cod parvalbumin. *Biophys. Chem.* 22:173–180.
23. Beece, D. L., H. Eisenstein, H. Frauenfelder, D. Good, M. C. Marden, L. Reinisch, A. H. Reynolds, L. B. Sorenson, and K. T. Yue. 1980. Solvent viscosity and protein dynamics. *Biochemistry*. 19:5147–5157.
24. Lakowicz, J. R., and G. Weber. 1973. Quenching of protein fluorescence by oxygen. Detection of structural fluctuations in proteins on the nanosecond time scale. *Biochemistry*. 12:4171–4179.
25. Calhoun, D. B., J. M. Vanderkooi, and S. W. Englander. 1983. Penetration of small molecules into proteins studied by quenching of phosphorescence and fluorescence. *Biochemistry*. 22:1533–1539.
26. Mayo, S. L., W. R. Ellis, R. J. Crutchley, and H. B. Gray. 1986. Long-range electron transfer in heme proteins. *Science (Wash. DC)*. 233:948–952.
27. Eftink, M. R., and C. A. Ghiron. 1984. Indole fluorescence quenching studies on proteins and model systems: use of the inefficient quencher succinimide. *Biochemistry*. 23:3891–3895.
28. Eftink, M. R., and C. A. Ghiron. 1976. Fluorescence quenching of indole and model micelle systems. *J. Phys. Chem.* 80:486–493.
29. Eftink, M. R., T. Selva, and Z. Wasylewski. 1987. Studies of the efficiency and mechanism of fluorescence quenching reactions using acrylamide and succinimide as quenchers. *Photochem. Photobiol.* 46:23–30.